AN AUTONOMOUS RECONFIGURABLE ANTENNA

A Thesis
Submitted to the Graduate Faculty
of the
North Dakota State University
of Agriculture and Applied Science

By

Lee Michael Hinsz

In Partial Fulfillment of the Requirements
for the Degree of
MASTER OF SCIENCE

Major Department:
Electrical and Computer Engineering

March 2019

Fargo, North Dakota

North Dakota State University
Graduate School

Title

AN AUTONOMOUS RECONFIGURABLE ANTENNA

By

Lee Michael Hinsz

The Supervisory Committee certifies that this ***disquisition*** complies with North Dakota State University's regulations and meets the accepted standards for the degree of

MASTER OF SCIENCE

SUPERVISORY COMMITTEE:

Dr. Benjamin D. Braaten
Chair

Dr. David A. Rogers

Dr. Erik Hobbie

Approved:

3/29/19
Date

Dr. Benjamin D. Braaten
Department Chair

ABSTRACT

Today's wireless communications involve more antenna capabilities while occupying the same amount of space. Antennas are able to operate at multiple frequencies [1]-[2], change polarizations [6], have selectable radiation patterns [1] and are becoming smaller. Likewise, antennas are serving multiple applications. However, many reconfigurable antennas use a separate power source to operate or use software defined radios. In certain instances this can be a limiting factor. To address this limit a novel autonomously reconfigurable antenna is presented in this thesis which allows for simple use at multiple frequencies [21]. This design uses power harvesting circuitry in combination with a reconfigurable antenna to demonstrate the ability to transmit at different frequencies, without the use of a separate power source. Furthermore this thesis presents a prototype for an autonomous reconfigurable antenna that operates at 1.25 GHz and 1.6 GHz.

TABLE OF CONTENTS

LIST OF FIGURES

LIST OF ABBREVIATIONS

AC .....Alternating Current

ADS.....Advanced Design Systems

BPF .....Band Pass Filter

Cos() .....Cosine function

DC .....Direct Current

dB .....Decibel

dBi.....Decibels relative to isotropic

dBm .....Decibels relative to milliwatts

fr .....Resonant frequency

G.....Gain

GHz.....Gigahertz

m .....Meters

MHz .....Megahertz

mm.....millimeter

mV.....millivolts

PCB.....Printed Circuit Board

pf .....Picofarads

PIN .....Positive Intrinsic Negative

Pr .....Power Received

RF .....Radio Frequency

Rin.....Input resistance to patch antenna

S11 .....Return Loss

S12 .....Insertion Loss

UWB.....Ultra Wide Band

VDC.....Voltage Direct Current

Vin.....Voltage Input

Vout.......................................Voltage Ouput

LIST OF SYMBOLS

ϵ_o .....Permittivity of free space

ϵ_r .....Dielectric Constant of substrate

ϵ_{reff}.....Effective Dielectric Constant

E_θ.....Electric Field in theta direction

f_{r1}.....Resonant frequency with PIN diodes off

f_{r2}.....Resonant frequency with PIN diodes on

h .....Height of substrate

P_{in} .....Power Input

λ .....Wavelength

ΔL .....Extension of antenna length

L_{eff} .....Effective antenna length

ς .....Tangent Loss

π.....Pi

yo.....Inset feed distance

μo.....Permeabilty of free space

vo.....Velocity of light in free space

W .....Width of patch and antenna

ZO .....Characteristic Impedance

CHAPTER 1. DESIGN (TOPOLOGY)

1.1. Project Overview

The reconfigurable antenna presented in this thesis is shown in Figure. 1, and uses an antenna involving a main and extended patch [21]. A power divider has an RF source connected to the input, one output connected to a reconfigurable antenna, and the second output connected to a power harvesting circuit. PIN diodes are used to change the topology of the patch antenna bridging the connection between the main and extended patch when the PIN diodes are active. To accommodate the tuning of the antenna with diodes on, a bandpass filter within the power harvesting circuit operates for selected frequencies. The filter then feeds a voltage-doubler circuit to apply voltage to a level high enough to bias the PIN diodes, and to rectify the AC source to DC. RF chokes are used to keep current from traveling back through to the voltage-doubler circuit and to isolate the characteristics of the antenna.

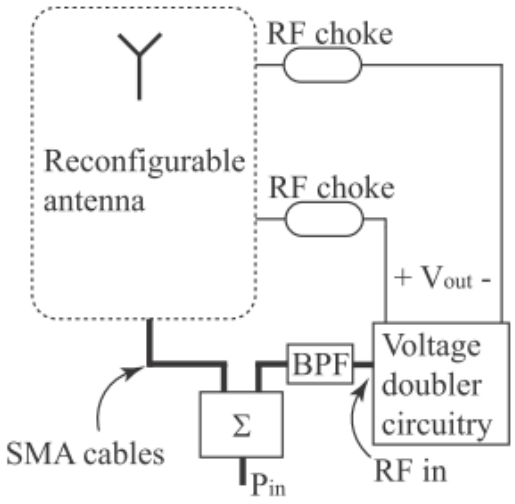

Figure 1. Topology of an autonomous reconfigurable antenna.

1.2. Power Divider

The purpose of the power divider in this project is to split the power and to provide matched ports for the reconfigurable antenna and power harvesting circuit [21]. A microstrip power divider is a microstrip configuration consisting of a metal ground plane, substrate, and metal top layer. A power divider is a microwave device that takes power and splits it across two ports and operates off principles of even and odd modes. Specifically for this project a Wilkinson power divider, shown in Figure. 2, is used and is made up of one input port and two output ports. The input feeds two symmetric branches consisting of a transmission line with a characteristic impedance $\sqrt{2} * ZO$ and a length equal to a quarter wavelength. A $2 * ZO$ ohm resistor terminates the branches at the end to complete the power divider. The transmission lines connected to both ports have a characteristic impedance of ZO.

The input port receives a signal from a source and one output port feeds the reconfigurable antenna and the other output port feeds a power harvesting circuit. This configuration offers benefits for the use of the project, such as less loss as the branches are non-resistive, and the output ports are well isolated.

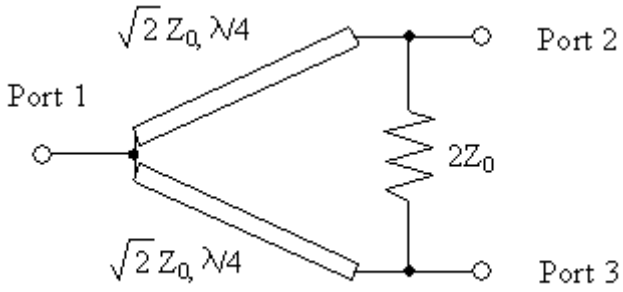

Figure 2. Illustration of Wilkinson power divider.

1.3. Reconfigurable Antenna

1.3.1. Microstrip Patch Antenna

A patch antenna consists of a metal patch surface on a substrate above a metal ground plane (as shown in Figure 3). The electric field exists between the ground plane and the top metal patch when fed from a source and the current propagates toward the far end of the patch from the source fed end. The physical length of the patch approximates the structures resonate frequency and as a good rule of thumb is selected to be $L_{approx} = \frac{vo}{2*f_r}$ with vo = velocity of light in free space, and f_r is equal to the desired resonant frequency of the antenna. The wavelength $\lambda = vo/fr$ and so the expression for the expression $L_{approx} = \lambda/2$. The width of the patch is calculated for radiation efficiency using the following [23]:

$$W = \frac{1}{2f_r\sqrt{\mu_o\epsilon_o}} * \sqrt{\frac{2}{\epsilon_r+1}} \quad (1.1)$$

With ϵ_r equal to the substrate dielectric.

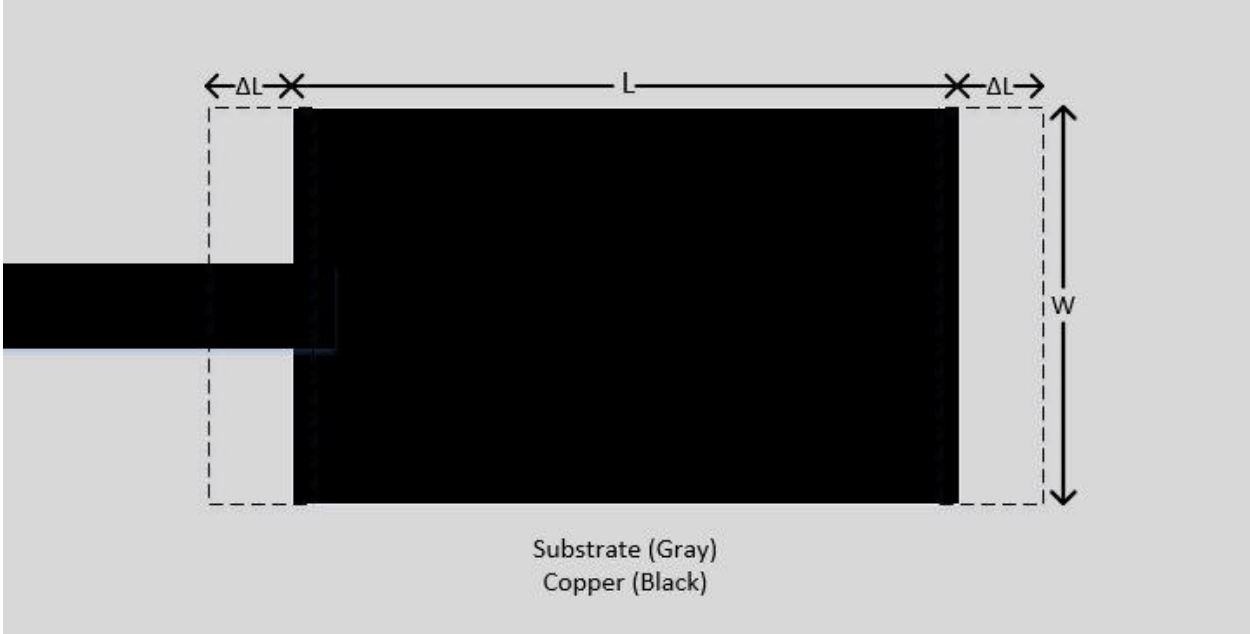

Figure 3. Patch antenna.

The substrate height (h) is made arbitrary and constant from the dimensions of the microstrip material. Based on the substrate height and two slots along the width of the patch there exists electric fields outside the top patch and substrate called fringe fields. These fields arc above the top copper, through air and then into the substrate to terminate on the ground plane. The path of the fringe fields change the dielectric constant since the electric field no longer exists only in the substrate. The effective dielectric constant (ϵ_{reff}) that accounts for the dielectric of air and of the substrate dielectric (ϵ_{r}) is approximated using [23]:

$$\epsilon_{\mathrm{reff}} = \frac{\epsilon_{\mathrm{r}}+1}{2} + \frac{\epsilon_{\mathrm{r}}-1}{2}\left[1 + 12 * \left(\frac{\mathrm{h}}{\mathrm{W}}\right)\right]^{-1/2}. \tag{1.2}$$

Equation 1.2 applies as long as $\frac{\mathrm{W}}{\mathrm{h}} > 1$. The fringe fields cause the electrical path to be longer than the physical length (L) of the patch such that the effective length is calculated using [23]:

$$\mathrm{L}_{\mathrm{eff}} = \mathrm{L} + 2 * \Delta\mathrm{L}. \tag{1.3}$$

To design a patch antenna that operates at a specific frequency and determine the physical length of the patch, the following equation needs to be solved for $\Delta\mathrm{L}$ [23]:

$$\frac{\Delta\mathrm{L}}{\mathrm{h}} = 0.412\frac{(\epsilon_{\mathrm{reff}} + 0.3)(\frac{\mathrm{W}}{\mathrm{h}} + 0.264)}{(\epsilon_{\mathrm{reff}} - 0.258)(\frac{\mathrm{W}}{\mathrm{h}} + 0.8)}. \tag{1.4}$$

The physical length (L) of the antenna can now be calculated using (1.3) and by rearranging the formula as [23]:

$$\mathrm{L} = \left(\frac{1}{2\mathrm{f}_{\mathrm{r}}\sqrt{\epsilon_{\mathrm{reff}}}\sqrt{\mu_{\mathrm{o}}\epsilon_{\mathrm{o}}}}\right) - 2 * \Delta\mathrm{L}. \tag{1.5}$$

To better match the impedance between the patch antenna and the microstrip feed line, an inset labeled as yo shown in Figure 4 is estimated for a desired input resistance using the following [23]:

$$\mathrm{Rin}(\mathrm{y} = \mathrm{yo}) \;=\; \mathrm{Rin}(\mathrm{y} = 0) \cdot \cos^2\left(\frac{\pi}{\mathrm{L}} \cdot \mathrm{yo}\right). \tag{1.6}$$

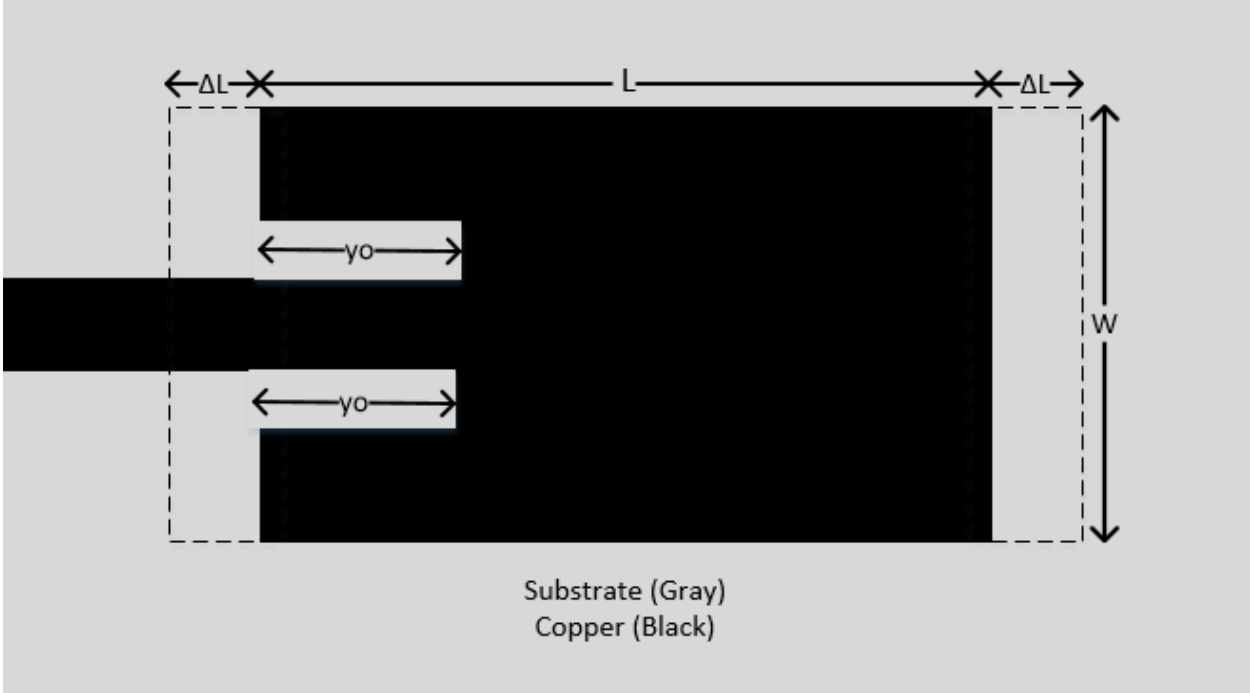

Figure 4. Recessed microstrip-line feed.

$\mathrm{Rin}(\mathrm{y} = 0)$ is resistance of the patch antenna without an inset, and is usually on the order of 300 ohms to 150 ohms. Formula 1.6 is used to estimate the approximate inset for yo as to provide a better match for the microstrip-line feed.

1.3.2. Reconfigurable Patch Antenna

For this work the antenna is reconfigurable by using an extended patch beyond the far end of the main patch and leaving a strip void of copper between the two patches. The copper void between the patches disconnects the two patches. The main patch length determines the first resonant frequency of the reconfigurable antenna while the extended and main patch combined length determine the second resonant frequency of the reconfigurable antenna. The resonant frequency of the main patch is f_{r1} and the resonant frequency of the main and extended combined patch is f_{r2}. The length of the combined extended and main patch will cause f_{r2} to be a lower frequency than f_{r1} due to the increased length. The length of the main patch is L_1 and the length of the combined patch is L_2 and is shown in Figure 5.

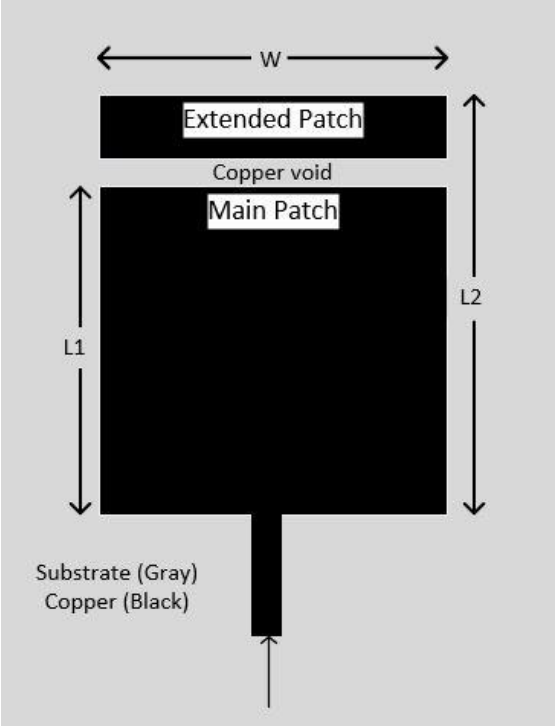

Figure 5. Main and extended patch reconfigurable antenna.

A number of PIN diode exists over the copper void to selectively bridge the connection between the main patch and extended patch. When PIN diodes are forward biased the electrical length of the

patch becomes longer relative to its length when PIN diodes are inactive. This produces a lower frequency when PIN diodes are active and higher frequency when inactive as shown in Figure 6. Or in other words a longer wavelength is supported when the diodes are on.

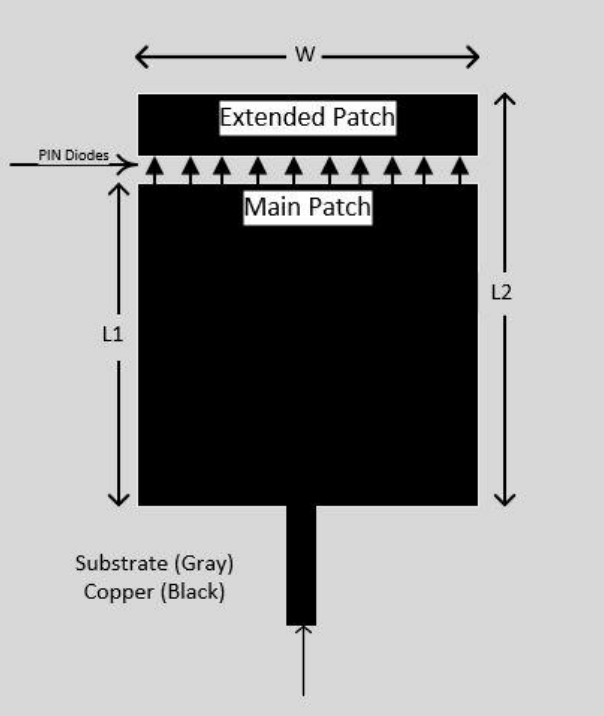

Figure 6. Main and extended patch with PIN diodes.

1.3.3. PIN Diodes

PIN diodes are used at microwave frequencies because of their low capacitance making them good RF conductors, with low turn-on voltage. These characteristics are ideal for the case of creating electrical bridges which have minimal impact on the impedance of the antenna. The low turn-on voltage and near zero resistance allows for efficient power use. A forward biased PIN diode has a resistance that becomes approximately zero thus allowing for almost no disturbance to the reconfigurable antenna, when the voltage applied is enough.

A PIN diode is made up of an intrinsic semiconductor region between a p-type semiconductor and an n-type semiconductor region. The semiconductor regions are shown in Figure 6. The p-type and

n-type regions are heavily doped because they are used for ohmic contacts. A PIN diode operates mainly like a standard diode at DC voltages and a near perfect resistor for frequencies above 1 GHz with enough forward bias voltage applied across it. The resistance value of the PIN diode is determined only by the forward biased dc current.

Figure 7. PIN diode illustration.

The RF voltage introduced from the RF source to the reconfigurable antenna is not enough to overcome the PIN diode threshold voltage, and is not constant, relative to VDC enough to bias the diodes due to the the DC voltage from the power harvester circuit, and so the PIN diodes do not react to the RF from the antenna source.

1.4. Power Harvesting

1.4.1. Band-pass Filter

A band-pass filter allows a certain range of frequencies to pass while blocking others. The method used to accomplish a band pass is through cascading a low pass and high pass filter together and the pass band is the overlapping pass bands of both filters. This is accomplished using two discrete surface mount components connected in series. The bandpass filter components are selected to allow f_{r2} to pass through to the voltage-doubler circuit and to block f_{r1}. The bandwidth of the filter needs to be narrow enough to allow the f_{r2} frequency band without allowing other frequencies to pass. Ideally the bandpass filter will only pass the frequencies desired for the power harvesting circuit, but because the design uses discrete, components predetermined low-pass and high-pass filter frequencies are used.

1.4.2. Voltage-Doubler Circuit

This circuit converts the voltage from AC to DC using a simple configuration of diodes and capacitors as seen in Figure 14 and in a schematic shown in Figure 8. The values in the schematic will be ignored for this section and be addressed in Section 2 (Prototype). The configuration of this circuit allows for full-wave rectification of the input signal. Specifically the circuit uses two schottky diodes arranged in a common anode configuration connected to two series capacitors attached to ground. The Vin comes from the bandpass filter and is from the source. During the positive voltage cycle, D1 is forward biased and charge is stored across capacitor C1. During the negative voltage cycle, D2 is forward biased and charge is stored in capacitor C2. Each cycle provides a sinusoidal voltage to PIN diodes and the ripple is smoothed out with the series capacitors. Schottky diodes were used for their response to higher frequencies and low losses to provide the most voltage to the PIN diodes of the reconfigurable antenna. The output voltage is taken across the two series capacitors and ideally the Vout will be two times Vin. The output voltage from this circuit is what allows the pin diodes to become active and thus make the antenna reconfigurable along with the source-fed frequency. This configuration was chosen for the minimum amount of components for populating a microwave circuit and since it doubles the voltage without influence of other parts of the design.

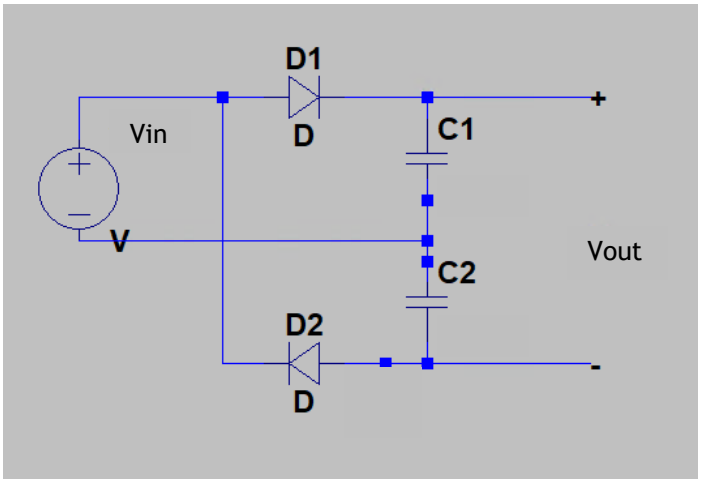

Figure 8. Voltage-doubler schematic.

CHAPTER 2. PROTOTYPE

A prototype of the project was designed, manufactured, and tested for results. Each component of the project was individually evaluated. The components of this project include a reconfigurable antenna with PIN diodes, power divider, a band-pass filter, and voltage-doubler circuit. The entire project was assembled and reviewed for demonstration and results.

2.1. Reconfigurable Antenna

The antenna was designed on a 0.7874 mm thick Rogers/Duroid 5880 [23] substrate (dielectric constant ε = 2.2 and loss tangent ς = 0.0004) and simulated in ADS [22]. The layout consists of a main patch antenna and an extended patch which while bridged is used for the lower frequencies or f_{r1}. A gap void of copper exists between the main patch and the extended patch. The gap is bridged with PIN diodes that were manufactured by Skyworks [24] (part number: SMP1322). RF chokes were manufactured by Mini-circuits [13] (part number: ADCH-80A) and are used to provide the control voltage to bias the PIN diodes and are attached to the conducting planes which allowed isolation from the ± VDC and the signal applied to the antenna. The main patch antenna operates at a higher frequency since the electrical length of the patch is smaller than the main and extended patch combined. When PIN diodes are biased the extended patch is part of the antenna and the electrical length of the antenna is longer. The feature of the reconfiguration occurs based on the voltage applied to the PIN diodes. When Vin to the PIN diodes is > 0 the PIN diodes are biased on and current conducts beyond the main patch to the extended patch [21]. When Vin of the PIN diodes is ~0 the PIN diodes are biased off and current is limited to the main patch. Thus the antenna operating frequency is higher for Vin ~0 and lower for Vin > 0. The prototype is show in Figure 9.

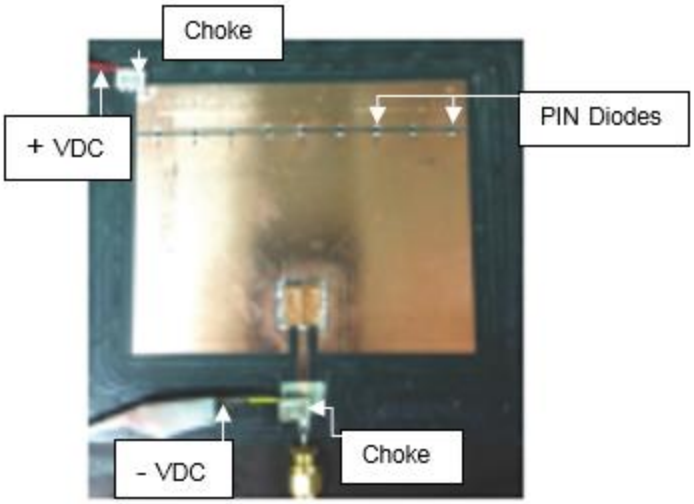

Figure 9. Prototype reconfigurable antenna.

Simulations were conducted in ADS to investigate the effects of PIN diodes on the reconfigurable antenna. For simulation purposes, 1 mm wide conductors were used to simulate each PIN diode biased to an ON state and is used to bridge the main patch and extended patch. The 1 mm conductors were removed to simulate the pin diodes biased OFF. S-Parameter and antenna gain results for a number of 1 mm conductors are show in Figure 10. The measurements were performed for N = 1,3,5,….13 PIN diodes evenly spaced across the main and extended patch. A complete conductor bridges the main and extended patch to assume that N approaches infinity and the best results possible for the extended patch operating. The results from these simulations indicate that for $N \geq 7$ a good gain and match can be achieved [21].

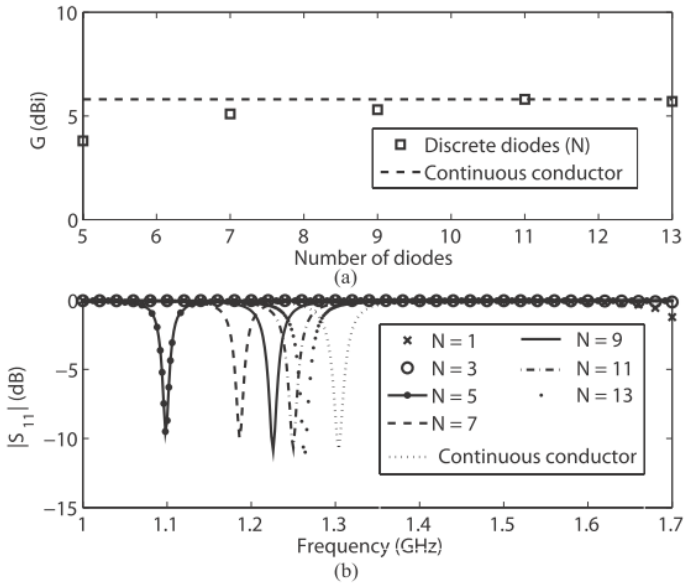

Figure 10. Simulated (a) gain and (b) S11 of antenna as PIN diodes are increased.

The antenna operating frequency was determined by evaluating the S11 simulation and measurement of the antenna for N = 9 PIN diodes. The result can be viewed in Figure 11.

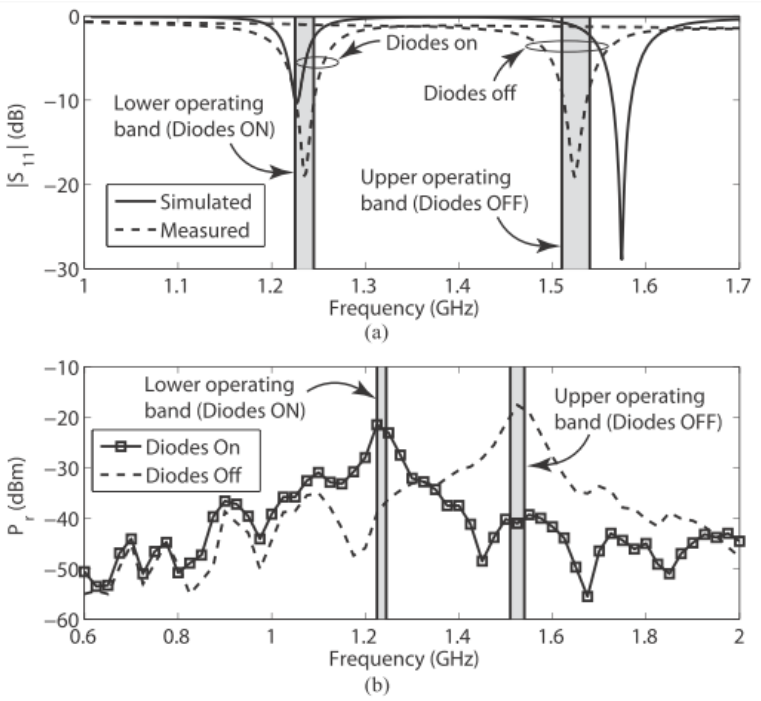

Figure 11. Simulated (a) and measured S-parameters of the reconfigurable antenna, (b) measured receive power of the reconfigurable patch antenna only at a distance of 2.0 m.

The simulated lower and upper -10 dB bands were 1.22 GHz to 1.23 GHz and 1.54 GHz to 1.60 GHz respectively, and the measured lower and upper -10 dB bands were 1.22 GHz to 1.245 GHz and 1.56 GHz to 1.58 GHz, respectively. The results agree very well in the lower operating band; however, the upper center frequency was simulated to be 1.574 GHz and measured to be 1.526 GHz. The difference between the measure and simulated center frequency of the band 1.56 GHz to 1.58 GHz is a result of reduced fringing field at the end of the main patch since the field does not extend as far due to the presence of the extended patch. Therefore more estimations could be considered for the effective dielectric calculations for the antenna design. Because the prototypes are used to demonstrate the proposed design in Figure 12, the measured -10 dB operating bands will be used. These bands are highlighted in grey in Figure 11 and throughout this thesis.

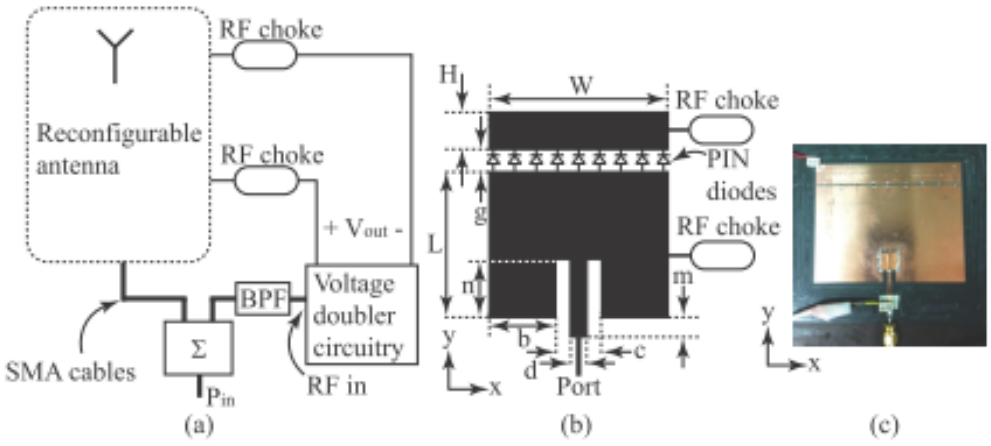

Figure 12. Layout (a) of the autonomous reconfigurable antenna for the use as a transmitter, (b) layout of the prototype reconfigurable antenna and (c) the manufactured reconfigurable microstrip antenna.

The gain of the antenna was measured in an anechoic chamber using the substitution method. This was done using two 1 – 18 GHz TDK horn antennas (model number:HRN-0118) 2.0 m apart and driving the transmit horn with 14.0 dBm of power with a function generator. The receive power for the field component E_θ was then measured with an Agilent EE4402B 3.0 GHz Spectrum Analyzer [14] at the receive horn in both operating bands. Low-loss 26.5 GHz micro-coax [15] SMA cables 4.5 m in length (part number: UFA210A-0-1800) were used to connect the TDK horn antennas to the function generator and spectrum analyzer. Then, the transmit horn being driven by the function generator was replaced by the reconfiguration patch prototype in Figure 12(c) and the receive power for the field component E_θ on the receive horn antenna was again measured at (0, 0, 2.0 m) in the anechoic chamber. Images for this setup are show in Figure 13(b). For the lower and upper operating bands, the gain was determined to be 0.5 dBi and 4.9 dBi, respectively. For these measurements an external DC voltage supply was connected to the RF chokes and used to switch the reconfigurable patch between the two frequency bands [21].

For comparison, the gain of the reconfigurable patch was simulated in ADS. The gain of the antenna in the lower and upper operating bands was computed to be 5.1 dBi and 5.6 dBi, respectively. The difference between the simulated and measured gains determined at the upper band are in part

due to the power absorbed by the unbiased diodes which can be seen in S11 measurements in Figure 13(a) and the PCB material losses. The difference between the simulated and measured gains at the lower band are believed to be due to the higher power absorption of the biased diodes, the PCB material losses and the low substrate thickness. The higher absorption of the diodes and substrate effect can be seen by comparing the measured receive powers in both bands in Figure 11(b) [21].

2.2. Band-pass Filter

The band-pass filter was designed in ADS on a 0.7874 mm thick FR4 substrate material (ε = 4.4 and loss tangent ς = 0.018) with conducting microstrip traces, ground plane, low pass-filter and high-pass filter surface mount components from Minicircuits [13] (low-pass filter part number: LCFN-1000 and high-pass filter part number: HFCN-740). The low-pass and high-pass filter components were connected in series. The low-pass filter has a cut-off frequency of 1275 MHz and the high-pass filter had a cut-off frequency of 780 MHz. A photograph of the bandpass filter is shown in Figure 13 along with measured and simulated S-parameters. It can be seen that the lower band of 1.23 GHz will pass and that the upper band will be blocked by the low-pass filter. Overall the high cutoff frequency of the filter was measured to be 1.29 GHz. This ensures that only the lower operating band will pass to the next stage of the design, being the voltage-doubler circuit, and will provide power to the PIN diodes of the reconfigurable antenna [21].

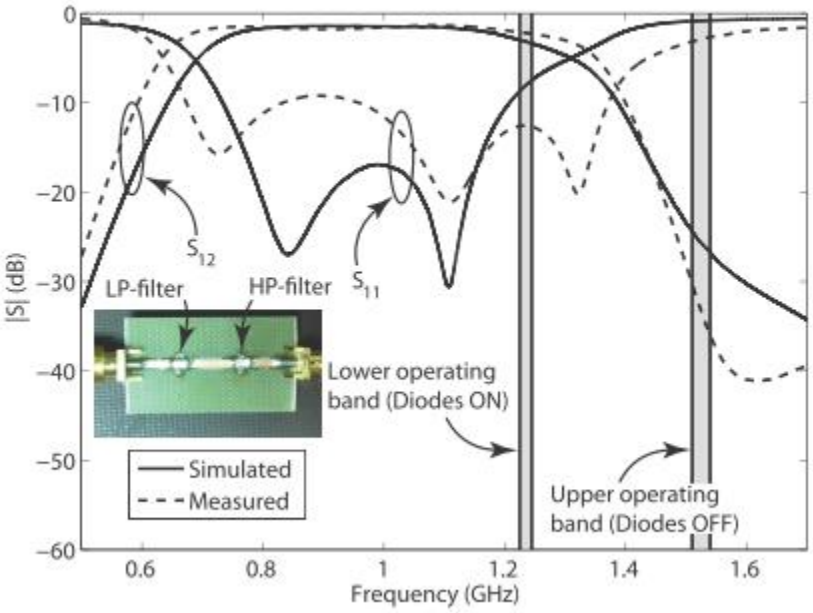

Figure 13. Simulated and measured S-Parameters of the band-pass filter.

2.3. Voltage-Doubler Circuit

Next, the voltage-doubler circuit and prototype board shown in Figure 14 were designed and tested. The diodes were manufactured by Avago Technologies [22] (part number: HSMS-2822-TR1G) and C1= C2= 470 pf for storing charge and allowing a small voltage ripple at frequencies when the circuit would be used. To test the performance of the circuit, an RF signal from a function generator was connected to the input of the band-pass filter with a 0.6 m low-loss Micro-coax cable [15] and the output of the filter was connected to the input of the voltage-doubler circuit which is N1 and N2, or Vin in Figure 14. A PIN diode was then connected between N3 and N4 and Vout was measured. The results are shown in Figure 14 for input powers of 10 dBm and 14 dBm. It can be seen that sufficient voltage is supplied through the bandpass filter and then by the voltage-doubler circuit to bias the PIN diodes of the reconfigurable antenna at the lower band and that the voltage is reduced at the upper band to unbias the diode [21].

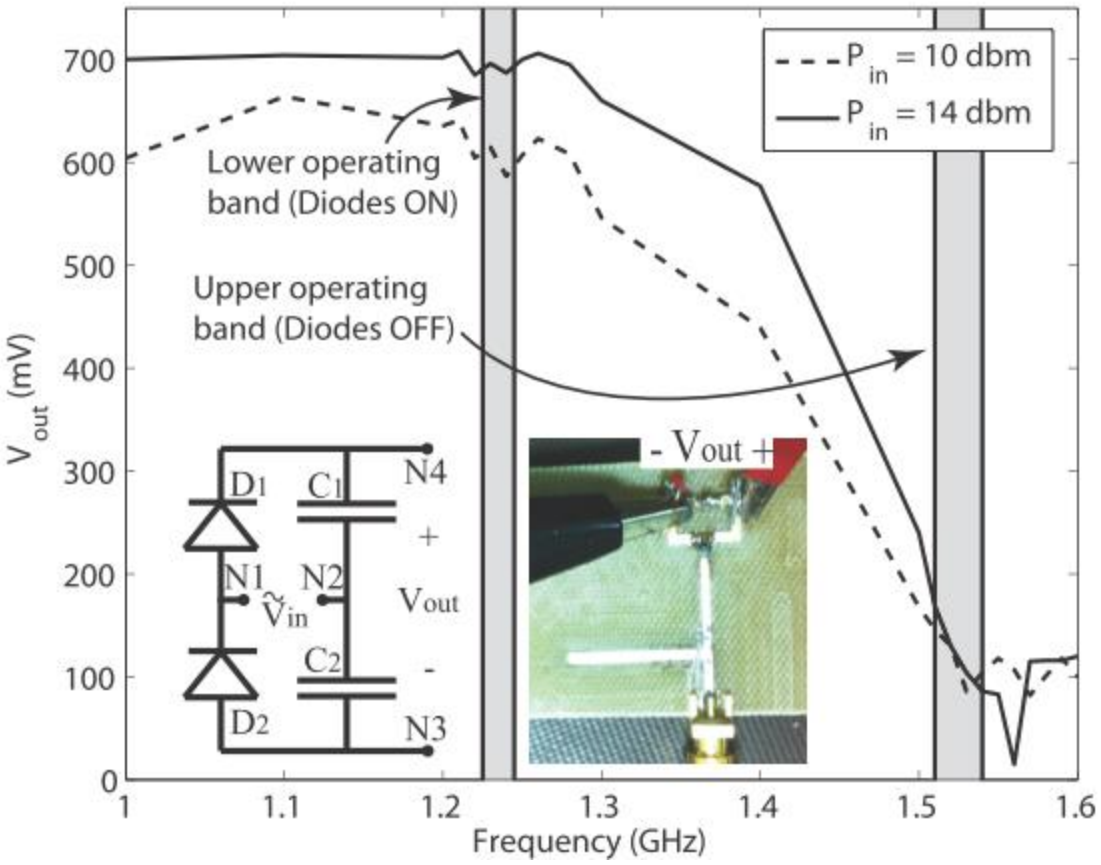

Figure 14. Voltage-doubler circuit.

2.4. Overall Antenna Performance

Lastly, for the overall demonstration of the prototype, the power divider, band-pass filter, voltage-doubler circuit and reconfigurable antenna were connected to make the assembly shown in Figure 15(a) [21]. The prototype was then placed in an anechoic chamber (shown in Figure 15(b)) and the radiated power was measured. The same function generator used to test the performance of the reconfigurable patch was used to drive the prototype antenna using the same 4.5 m Micro-coax cable. A TDK 1-18 GHz horn antenna was connected to an Agilent E4402B 3.0 GHZ Spectrum Analyzer again using the same 4.5 m Micro-coax cable as before, and E_θ of the radiated field was measure at (0,0, 2.0 m).

Initially, to determine that the PIN diodes were being fully biased by the voltage-doubler circuitry in the lower band, the input power was increased from 0 dBm to 16 dBm in steps of 2.0 dBm. The receive power was then measured for each of these input power values and the results are shown in Figure 16(a) at 1225 MHz. A noticeable increase in power occurs at 8 dBm, indicating that the PIN diodes are beginning to be biased. Next to determine when the diodes were fully biased, the wires connecting the diodes to the voltage-doubler circuit were disconnected and reconnected to a DC voltage supply. The power divider, band-pass filter and voltage-doubler circuit were left intact in the chamber and the diodes were now biased by an external voltage supply. The DC voltage was set to 400 mV and then 700 mV, and the received power was measured in a similar manner. By setting the voltage to 400 mV, the diodes were unbiased and by increasing the voltage to 700 mV, this ensured fully biased PIN diodes and a max radiated field in the lower band. The results from these measurements are shown in Figure 16(b). When comparing the voltage-doubler curve to the receive power values measured for VDC = 400 mV and 700 mV, it can be seen that when the input power is at 14 dBm, the diodes are fully biased by the voltage-doubler circuit.

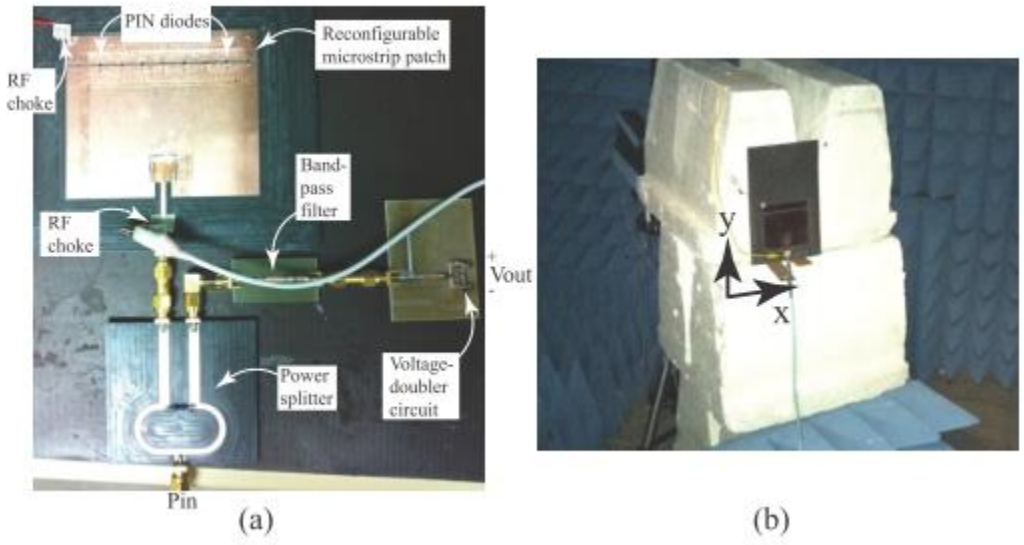

Figure 15. Picture (a) of the prototype antenna and (b) picture of the prototype antenna being measured in the anechoic chamber (in the x-y plane).

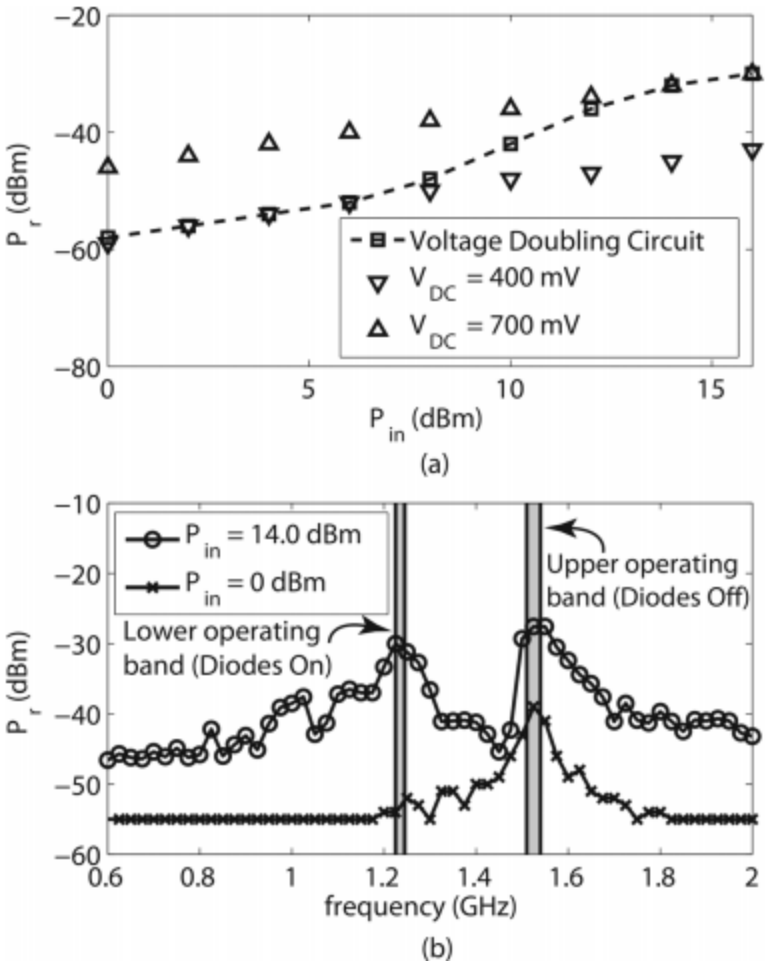

Figure 16. Comparison (a) of the measured receive power at 1225 MHz of the prototype antenna when the PIN diodes are biased by the voltage-doubler circuit and a DC voltage supply and (b) measured receive power of the prototype antenna at a distance of 2.0 m with PIN biased by the voltage-doubler circuit.

Finally, the diodes were reconnected to the voltage-doubler circuit and the input frequency was swept from 600 MHz to 2.0 GHz. The radiated power was then measured at (0,0, 2.0 m) and the results from these measurements are shown in Figure 16(b) [21]. The input powers were used to demonstrate that the diodes were switching on at the lower band. For an input power Pin of 0 dBm, radiated power was only observed at the upper operating band which occurs when the diodes are unbiased (as shown in Figure. 16(a)). P_{in} was then raised to 14.0 dBm to provide enough power to bias the PIN diodes.

Next, using the measured received power values, the gains for the lower and upper bands were determined to be –4.0 dBi and 1.0 dBi, respectively. Furthermore, comparing the received power values of the prototype in Figure 16(b) to the received power values of the reconfigurable patch in Figure 11(b), a reduction of 4.5 dBm and 3.9 dBm is shown in the lower and upper bands, respectively. These reductions in power are due to the introduction of the power divider and connectors into the measurements, and the additional loss in the lower band is believe to be due to the PIN diodes. Another consideration regarding the difference in the upper band received power is due to less fringe fields, since the extended patch of the reconfigurable antenna block the ability for the field to terminate on the ground plane.

For an analytic comparison, the Friis equation was used next to compute the efficiency of the prototype antenna. Using the measured gains of the reconfigurable patch antenna in the previous section, the expected receive power was computer to be Pr = -19.3 dBm and -15.3 dBm in the lower and upper bands, respectively. This then results in a computed power absorption of 3.8 dBm by the power divider, filter and voltage-doubler circuit in both bands. The Wilkinson power divider is expected to cause a 3 dB difference due to an even power split. This compares to the previously measured absorption of 4.5 dBm and 3.9 dBm in the lower and upper bands respectively.

Finally, the S11 values were measured using an Agilent E5071C 100 kHz-8.5 GHz ENA series Network Analyzer [14]. The output of the network analyzer was set to 10 dBm (max allowable value) and the sweep time was set to 20 seconds. This longer sweep time ensured that the voltage-doubler circuit was enabled and the diodes were beginning to be biased. The results from these measurements gave $S11$ = -14.0 dB and -19.0 dB in the lower and upper bands, respectively.

CHAPTER 3. RESULTS

3.1. Discussion

The prototype in Figure 15(a) was meant to demonstrate the antenna topology presented in Figure 12(a), and many new designs could be developed to improve the performance of the prototype antenna. Further optimization of the design could include an arbitrary power splitter, using switches with less loss, antenna arrays, substrate with lower loss tangents than FR4, thicker substrates for the operating bands chosen in this work, amplifiers to overcome the loss of the circuitry and integration of the entire antenna on a single substrate [21]. However, the results in Figure 16(b) show that the microstrip antenna is autonomously reconfigurable and radiating in the desired bands.

Several applications of the antenna presented in this work were mentioned earlier. One application could be the replacement of numerous multiband antennas in multistandard-radio base stations with a single autonomous reconfigurable antenna. For comparison, the designs reported in [16]-[19] have gain values that vary from -4 dBi to +4dBi and the geometries range from half the sizes comparable to the antenna designed in this thesis. The concept of autonomous switching proposed in this thesis could be used to replace at least two of these with a single design, saving space and having comparable gain values. Furthermore, the concepts could be extended to replacing more than two antennas with a single design.

The second application mentioned was related to replacing two orthogonal Yagi antennas and cables with a single reconfigurable antenna and one cable. In some long-distance wireless sensor applications, two coaxial cables are attached to an antenna mast to drive each Yagi antenna. This, one antenna is used to communicate in one direction with a vertical linear polarization and one antenna is used to communicate in the same direction with a horizontal linear polarization in a different operating band. By using an autonomous polarization [6] reconfigurable antenna instead of two Yagi antennas, a cable and antenna could be completely removed from the antenna mast.

Finally, the third application commented on was the replacement of an UWB antenna. In some applications, the gain of an UWB antenna (such as a spiral) can be as low as -15 dBi below resonance and up to 5 dBi above resonance [20]. However, the entire bandwidth of the spiral antenna may not be

needed by a multi-band system and a reconfigurable antenna could be used. Also, a separate control signal may not be available in the existing system that uses a spiral antenna. By implementing the design in this thesis, the gain at the desired frequencies could be improved to values above -15 dBi without the requirement of a control signal.

CHAPTER 4. CONCLUSION

An autonomous reconfigurable antenna has been presented and demonstrated. More specifically, the proposed antenna uses RF circuitry to convert a portion of the input power to a DC voltage over a specific operating band. This DC voltage is then used to bias PIN diodes embedded in a reconfigurable antenna. Thus, when the antenna is driven in a specific band, the diodes are biased and when the antenna is driven out of the designed band, the diodes are unbiased. For demonstration purposes, a prototype antenna with RF circuitry and a reconfigurable microstrip antenna was manufactured and tested. Overall, it was shown that the antenna could autonomously switch between two states without the requirements of a control signal. This makes this antenna design very useful for new and existing systems that would benefit from the uses of a reconfigurable antenna.

BIBLIOGRAPHY

[1] S. Nikolaou, R. Bairavasubramanian, C. Lugo Jr, I. Carrasquillo, D.C. Thompson, G.E. Ponchak, J. Papapolymerou, and M.M. Tentzeris, "Pattern and Frequency Reconfigurable Annular Slot Antenna Using PIN Diodes," IEEE Transactions on Antennas and Propagation, Vol. 54, No. 2, p. 439-448, February 2006.

[2] D.E. Anagnostou, and A.A Gheethan, "A Coplanar Reconfigurable Folded Slot Antenna Without Bias Network for WLAN Applications," IEEE Antennas and Wireless Propagation Letters, Vol. 8, p. 1057-1060, October 2009.

[3] S.-L.S. Yang, A.A. Kishk, and K.-F. Lee, "Frequency Reconfigurable U-Slot Microstrip Patch Antenna," IEEE Antennas and Wireless Propogation Letters, Vol. 7, p. 127-129, January 2008.

[4] S. Weigand, K.H. Pan, and J. T. Bernhard, "Analysis and Design of Broad-Band Single-Layer Rectangular U-Slot Microstrip Patch Antennas," IEEE Transactions on Antennas and Propagation, Vol. 51, No. 3, p. 457-468, March 2003.

[5] S. Xiao, B.-Z. Wang, and X.-S. Yang, "A Novel Frequency-Reconfigurable Patch Antenna," Microwave and Optical Technology Letters, Vol. 36, No. 4, P. 295-297, February 20 2003.

[6] K. Chung, Y. Nam, T. Yun, and J Choi, "Reconfigurable Microstrip-Patch Antenna with Frequency and Polarization-Diversity Function," Microwave and Optical Technology Letters, Vol. 47, No. 6, p. 605-607, December 2005.

[7] F. Yang and Y. R.-Samii, "Patch Antenna With Switchable Slot (PASS): Dual-Frequency Operation," Microwave and Optical Technology Letters, Vol. 31, No. 3, p. 165-168, November 2001.

[8] N. Jin, F. Yang, and Y.R-Samii, "A Novel Patch Antenna With Switchable Slot (PASS): Dual-Frequency Operation with Reversed Circular Polarizations," IEEE Transactions on Antennas and Propagation, Vol. 54, No. 3, p. 1031-1034, March 2006

[9] H. Chen, Z. Shi, L. Wu, and D. Guo, "Frequency Reconfigurable Antenna with Micromechanical Patch," IEEE Transactions on Antennas and Propagation, Vol. 46, No. 11, p. 18-22, 1998.

[10] Z. Alam and R. Islam, "Reconfigurable Patch Antenna by RF MEMS Switches,"Proceedings of the 6th International Symposium on Mech atronics and its Applications, Sharjah, 1998, pp.1-3.

[11] G. Zhang, J. Hong and B. Wang, "A novel pattern reconfigurable wideband slot antenna using PIN diodes," 2010 International Conference on Microwave and Millimeter Wave Technology, Chengdu, 2010, pp. 22-24.

[12] Q. Chen, M. Kurahashi and K. Sawaya, "Dual-mode patch antenna switched by PIN diode," 2003 IEEE Topical Conference on Wireless Communication Technology, Honolulu, HI, USA, 2003, pp. 148-149.

[13] Mini-circuits [Online]. Available: www.minicircuits.com

[14] Agilent Technologies [Online]. Available: www.agilent.com

[15] Micro-coax [Online]. Available: www.micro-coax.com

[16] K. Wong and L. Lee, "Multiband Printed Monopole Slot Antenna for WWAN Operation in the Laptop Computer," in IEEE Transactions on Antennas and Propagation, vol. 57, no. 2, pp. 324-330, Feb. 2009.

[17] T.-W. Kang and K.-L. Wong, “Internal printed loop/monopole combo antenna for LTE/GSM/UMTS operation in a laptop computer,” Microw. Opt. Tech. Lett., vol. 52, no. 7, pp. 1673–1678, Jul. 2010.

[18] L. Chou and K. Wong, "Uni-Planar Dual-Band Monopole Antenna for 2.4/5 GHz WLAN Operation in the Laptop Computer," in IEEE Transactions on Antennas and Propagation, vol. 55, no. 12, pp. 3739-3741, Dec. 2007.

[19] Songnan Yang, A. E. Fathy, S. M. El-Ghazaly and V. K. Nair, "Novel reconfigurable multi-band antennas for multi-radio platforms," 2008 IEEE Radio and Wireless Symposium, Orlando, FL, 2008, pp. 723-726.

[20] Printed Antennas for Wireless Communications, R. Waterhouse, Ed. West Sussex, U.K.: Wiley, 2007.

[21] L. Hinsz and B. D. Braaten, "A Frequency Reconfigurable Transmitter Antenna With Autonomous Switching Capabilities," in *IEEE Transactions on Antennas and Propagation*, vol. 62, no. 7, pp. 3809-3813, July 2014.

[22] Avago Technologies [Online]. Available: www.micro-coax.com

[23] Constantine A. Balanis, “Antenna Theory,” 3rd Ed., John Wiley and Sons, Inc., Hoboken, New Jersey, 2005, p.817-825.